

RSC Advances



This is an *Accepted Manuscript*, which has been through the Royal Society of Chemistry peer review process and has been accepted for publication.

Accepted Manuscripts are published online shortly after acceptance, before technical editing, formatting and proof reading. Using this free service, authors can make their results available to the community, in citable form, before we publish the edited article. This *Accepted Manuscript* will be replaced by the edited, formatted and paginated article as soon as this is available.

You can find more information about *Accepted Manuscripts* in the [Information for Authors](#).

Please note that technical editing may introduce minor changes to the text and/or graphics, which may alter content. The journal's standard [Terms & Conditions](#) and the [Ethical guidelines](#) still apply. In no event shall the Royal Society of Chemistry be held responsible for any errors or omissions in this *Accepted Manuscript* or any consequences arising from the use of any information it contains.

Cite this: DOI: 10.1039/c0xx00000x

www.rsc.org/xxxxxx

ARTICLE TYPE

Fabrication of Nanostructured V₂O₅ via Urea Combustion for High-performance Li-ion Battery Cathode

Qiang Song,^a Hongchang Pang,^a Weitao Gong,^a Guiling Ning^{*a}, Song Gao,^b Xinglong Dong,^b Chunjing Liu,^b Junying Tian^a and Yuan Lin^a

Received (in XXX, XXX) Xth XXXXXXXXX 20XX, Accepted Xth XXXXXXXXX 20XX
DOI: 10.1039/b000000x

The nanostructured vanadium pentoxide (V₂O₅) crusts are facilely synthesized *via* combustion of precursor from mixing commercial V₂O₅ with molten urea. And the nanocrusts can be transferred to nanorods during the further annealing at 630 °C. Both of the V₂O₅ nanocrusts and V₂O₅ nanorods have been preliminarily used as cathode material for Li-ion Battery. The electrode performance of them is highly improved in comparison with commercial V₂O₅.

Vanadium pentoxide (V₂O₅) has drawn much attention due to its great potentiality in a variety of applications such as electrode materials in solid state batteries and supercapacitors.¹⁻⁶ Specially, V₂O₅ is one of the most promising cathode material for high energy density Li-ion battery owing to its high theoretical capacity (440 mA h g⁻¹ with three lithium insertions/extractions), which is much higher than those of more widely used cathode materials such as LiCoO₂ (140 mA h g⁻¹), LiMnO₂ (148 mA h g⁻¹), LiFePO₄ (170 mA h g⁻¹).⁵⁻⁸ V₂O₅ also has the additional advantages of inexpensive and abundant. However, the slow diffusion of lithium ions (D~10⁻¹² cm² s⁻¹) and low electronic conductivity (10⁻² to 10⁻³ S cm⁻¹) of commercial V₂O₅ crystals impede them to act as high-performance electrode materials for Li-ion battery in large scale production.⁷⁻¹⁰ Recently, many literatures indicate that nanostructures of electrode materials are able to improve the performance due to the dimension reduction of particles size, which shortens the lithium ions' diffusion and electron transportation.⁹⁻¹¹

Up to now, various V₂O₅ materials with different nanostructures such as nanorods, nanofibers, nanowires and nanobelts have been prepared by chemical methods such as hydrothermal growth, sol-gel synthesis and flame spray-pyrolyzed.⁸⁻¹⁵ For instance, nanorod structured V₂O₅ synthesized by thermal decomposition of vanadium precursors, exhibiting a good performance of discharge capacity and cycle stability as cathode for Li batteries.⁹ In addition, nanorods, nanowires and nanobelts have also been obtained by thermal evaporation, sputtering deposition and recrystallization, although the products of these methods mainly are thin layers on substrates.^{16, 17} V₂O₅ nanorods have been fabricated *via* long time ball milling and annealing by Glushenkov et al., giving a stable electrochemical performance as cathode for Li batteries.¹⁶ So far right now, it is always highly focused on developing a convenient method which could be applied to produce V₂O₅ nanomaterials in large scale production. Thus, a novel cost-effective method producing V₂O₅

nanomaterials with high performance for Li-ion battery is of great need.

In this study, we report a novel and convenient approach capable of producing nanostructured V₂O₅ crusts (nanocrusts), which is feasible for mass production. The V₂O₅ nanocrusts composed of nanoparticles is fabricated *via* direct combustion of a black precursor at 450 °C in air for an hour. And the black precursor was obtained by commercial V₂O₅ reacting with molten urea at a starting mass ratio of 1 : 4 at 140 °C for 30 min. Herein, urea is not only the combustion agent but also the reagent for the reaction of V₂O₅ at preprocessing.^{18, 19} And V₂O₅ nanorods are obtained by a recrystallization process in further annealing at 630 °C. Electrochemical performance of as-prepared V₂O₅ electrode materials for Li-ion battery has been demonstrated, exhibiting high-rate charge/discharge capacity and good cycle stability.

The photograph of the black precursor *via* the reaction of commercial V₂O₅ and molten urea is shown in Figure S1a. The colour of the melt mass gradually changed from yellow (commercial V₂O₅) to black, indicating that the V₂O₅ had been reacted with molten urea. The colour of the melt mass gradually changed from yellow (commercial V₂O₅) to black, indicating that the V₂O₅ had been reacted with molten urea. The FT-IR spectrum of the black precursor is shown in Figure S2. The bands at about 3461, 3340, 2226, 1682, 1605, 1466, 1338, 1156, 981 and 574 cm⁻¹ are indexed to black precursor. The bands at 1682 and 1466 cm⁻¹ are ascribed to stretching vibration of C=O and C-N, while those bands at 3461, 3340 and 1605 cm⁻¹ can be assigned to asymmetric, symmetric stretching and deformation vibration of N-H bonds, respectively. And the band at 1156 cm⁻¹ can be attributed to rocking vibration of NH₂. These can be owing to the presence of unreacted urea in the black precursor. The absorption at 981 cm⁻¹ should be associated with the V=O band, which is related to vanadic complex after the reaction of V₂O₅ and molten urea.^{20, 21} But all of the three major absorption peaks of V₂O₅ at 617, 827, and 1022 cm⁻¹ are invisible in the spectrum (Figure S1a).²² Moreover, the bands at 2226 and 1338 cm⁻¹ can be ascribed to the absorptions of -N=C=O. These indicate that V₂O₅ has completely reacted with urea.²⁰⁻²²

Thermal decomposition behaviour of the precursor was investigated by thermal gravimetric (TG) analysis. Figure S3 shows the TG results for the black precursor calcined in air. Two distinct stages were observed. The sharp weight loss around 200 °C in the first stage can be attributed to the condensation and

deamination of urea in the mixed precursor.¹⁸ Then a steep slope indicating another weight loss at 405 °C is observed, which demonstrated the successful thermal-decomposition of vanadate to vanadium oxide. And the weight of final production is correspond to the V₂O₅ in initial mass ratio.¹⁹

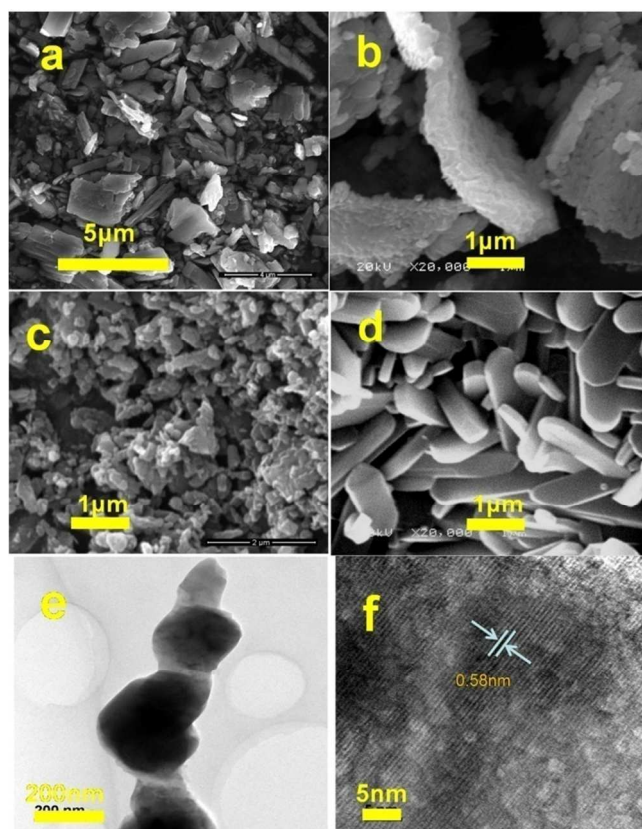


Figure 1 Morphologies and structural information of V₂O₅ particles: (a) SEM image of commercial V₂O₅; (b) SEM image of the sample synthesized by thermal decomposition of the black precursor (the starting mass ratio of V₂O₅ to urea is 1 : 4) at 450 °C for 1h; (c) SEM image of the sample after subsequent annealing in air at 630 °C for half an hour; (d) SEM image of the sample has been ground into individual particles; (e) TEM image of the sample has been ground into individual particles; and (f) high-resolution transmission electron microscopy (HRTEM) image of individual particles.

The micro morphologies and structures of commercial V₂O₅ and the V₂O₅ nanocrusts are shown in Figure 1a and 1b. As shown in Figure 1a, the commercial V₂O₅ is micrometer-sized particles with irregular shapes. The yellow bread-like product with foam structure (see Figure S1b and S1c) is obtained by calcinating the black precursor in air at 450°C for 1 h. Figure S1c shows that the foam structure consists of nanostructured crusts (nanocrusts) during combustion. Figure 1b indicates V₂O₅ nanocrusts are composed of nanoparticles. Furthermore, elongated nanorods have been formed by further annealing nanocrusts in air at 630 °C (Figure 1d). The nanocrusts can also be crushed into individual nano-sized particles by grind. The morphology and structure of the nanoparticles obtained by simply grinding the nanocrusts are shown in Figure 1c and 1e, illustrating the sizes of particles range from 50 nm to 300 nm. Figure 1f shows a high resolution TEM image of a part of the nano-sized V₂O₅ particles, revealing a layer structure of V₂O₅. And the lattice fringes with spacing of 0.58 nm

should be correspond to the (200) planes of orthorhombic V₂O₅.²³

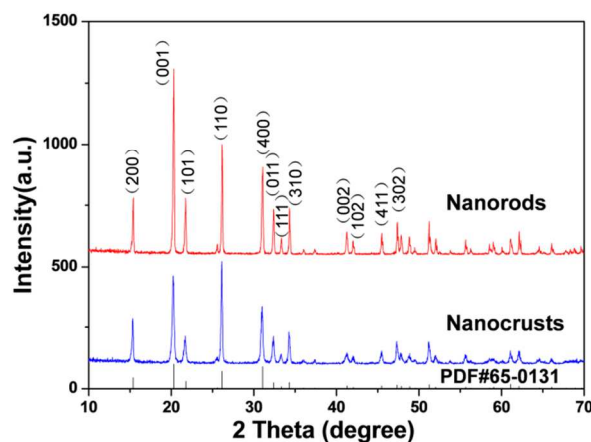


Figure 2 Powder X-ray diffraction (XRD) patterns of the nanocrusts synthesized *via* thermal decomposition of black precursor (the starting mass ratio of V₂O₅ to urea is 1:4) at 450 °C for an hour and the nanorods obtained by annealing the nanocrusts in air after subsequent at 630 °C for 30 min. The vertical lines indicate the peak positions expected for orthorhombic V₂O₅ from JCPDS Card No. 065-0131.

The phase and purity of as-prepared nanocrusts and nanorods were determined by powder X-ray diffraction (XRD). The diffraction patterns are displayed in Figure 2. Both of them can be indexed well to a monocline structure V₂O₅ space group with the space group : *P21/c*, *a* = 11.512 Å, *b* = 3.564 Å, *c* = 4.368 Å (JCPDS Card No. 65-0131), showing the high phase purity of the nanocrusts and the nanorods. Meanwhile, the peaks of the V₂O₅ nanocrusts are weaker and wider than that of the V₂O₅ nanorods, especially the relative intensity of (001) peak, which suggests that nanorods have better crystallinity and bigger particle size. The crystallite dimensions of nanocrusts and nanorods can be calculated from the (001) peak *via* Scherrer equation. The V₂O₅ nanocrusts (36.7nm) is much smaller than the V₂O₅ nanorods (78.5nm).^{9, 16}

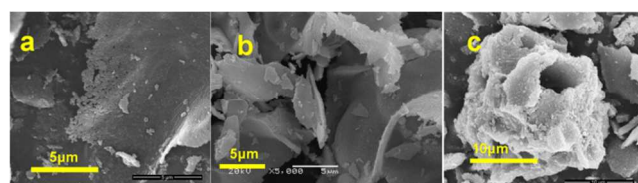
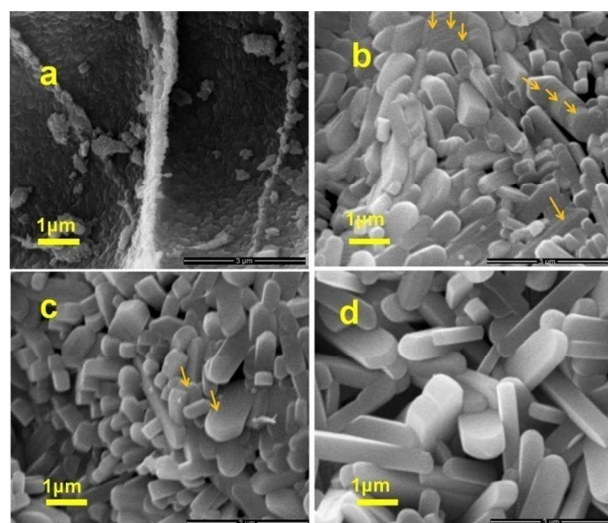


Figure 3 SEM images of the V₂O₅ nanocrusts synthesized by thermal decomposition of the black precursor with different starting molar ratios of V₂O₅ to urea: (a) 1:5; (b) 1:4; (c) 1:3.

The morphologies of the products obtained from different urea contents in the starting reagents are shown in Figure 3. Figure 3a and 3b show the SEM images of the samples produced by thermal decomposition at 450 °C for 1h with the mass ratio of V₂O₅ to urea were 1: 5 and 1 : 4, respectively. The morphologies of the samples are nanocrusts assembled from nanoparticles. However, the nanostructured crusts cannot be obtained in the 1 : 3 V₂O₅ products (mass ratio of V₂O₅ to urea is 1 : 3). Instead, micro-aggregates have been obviously observed (Figure 3c). It could be considered that V₂O₅ bread could be formed eventually with excess urea decomposition during calcination process. And the nanocrusts are the bubble walls in V₂O₅ bread. Therefore, the

thinner crust would be achieved in higher urea mass ratio, because formation of more gas from urea decomposition leads to bigger bubbles and thinner walls in V_2O_5 bread.



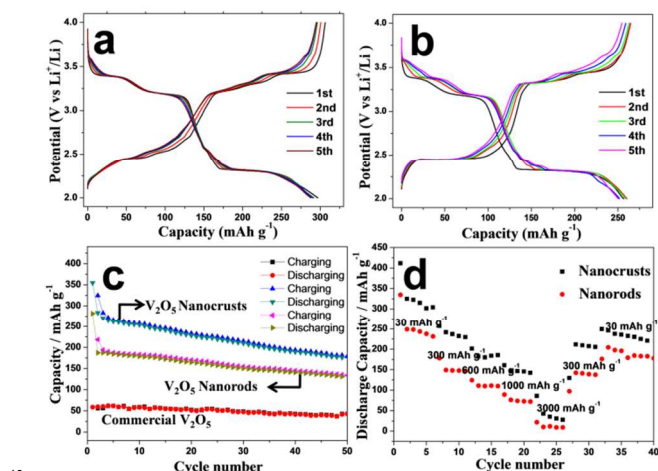
5 Figure 4 The transformation of the nanocrusts into nanorods: (a) SEM image of the surface of the V_2O_5 nanocrusts synthesized by thermal decomposition of the black precursor (the starting mass ratio of V_2O_5 to urea is 1 : 4) at 450 °C for 1h; the V_2O_5 nanocrusts after subsequent annealing in air at 630 °C for 5, 10 and 30 min (b, c and d respectively).
10 Formation of new layers on existing {001} surfaces are shown with arrows in b and c.

The shapes transformations of the V_2O_5 nanocrusts by further annealing progress at 630 °C are shown in Figure 4. The SEM image in Figure 4a shows that the surface of the nanocrusts consists of nanoparticles with irregular shapes. And the SEM images in Figure 4b, 4c and 4d reveal the morphology changes of nanocrusts after 5, 10, and 30 min of annealing treatment. The shapes of the powders are almost completely transformed from nanocrusts to nanorods after 30min annealing. These nanorods look like ice cream sticks which have a round end and rectangular cross section. The width of the rods grown after 5 min was in the range of 300 – 800 nm. The thickness was between 100 and 300 nm. And the length was up to several micrometers. According to the reported work of Glushenkov et al.¹⁶, the formation and growth of nanorods can be ascribed to a surface energy driven recrystallization process. The morphology of nanorods is a particular type of facets which dominated by notable low energy {001} surfaces (by calculation)²⁴. As shown in Figure 4b and 4c, it can be observed that new layers (shown with arrows) formed on the {001} surfaces in nanorods growth process.¹⁶ Meanwhile the nanocrusts provide enough space for particles growth to elongated nanorods, preventing the formation of larger crystal due to the coalescence behaviour on adjacent nanorods.

This method involving reaction between commercial V_2O_5 and molten urea and annealing in a muffle furnace is easy to produce real mass quantities of materials with nanostructure. And the products can be broken to nanocrusts, nanoparticles or nanorods by ball milling. If required, materials with various particle sizes can be separated by sieving. It is demonstrated that both roasting technology and mechanical milling can be easily capable of scaling up.

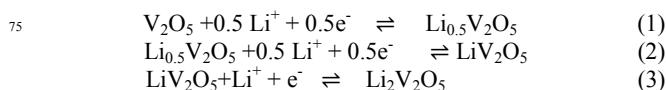
Considering the Li-ion storage performance of commercial

V_2O_5 , we investigated the application in a Li ion battery (LIB) as a proof-of-concept demonstration of their potential use.



45 Figure 5 Electrochemical testing of the V_2O_5 materials as the cathodes in $LiPF_6$ electrolyte: The 1st to 5th charge–discharge profiles of (a) the V_2O_5 nanocrusts synthesized *via* thermal decomposition of black precursor (the starting mass ratio of V_2O_5 to urea is 1.4) at 450 °C for 1h and (b) the V_2O_5 nanorods obtained by the V_2O_5 nanocrusts after subsequent annealing in air at 630 °C for half an hour in the voltage range of 2.0 – 4.0 V at a rate of 30 mA g⁻¹; (c) Cycling performances of commercial V_2O_5 , the V_2O_5 nanocrusts and the V_2O_5 nanorods in the voltage range of 2.0 – 4.0 V at a rate of 300 mA g⁻¹; (d) The rate performances of the V_2O_5 nanocrusts and the V_2O_5 nanorods in the voltage range of 2.0 – 4.0 V.
50
55

Galvanostatic charge–discharge measurements were performed on the V_2O_5 nanocrusts and the V_2O_5 nanorods at a current density of 30 mA g⁻¹ between 2.0 – 4.0 V. The initial five charge–discharge profiles for these measurements are illustrated in Figure 5a and 5b. Both of the nanocrusts and nanorods showed three characteristic plateaus at the voltages of about 3.4, 3.2 and 2.3 V (vs. Li/Li^+) in those discharge curves. These plateaus are corresponding to the phase transformation of crystalline α - V_2O_5 to α - $Li_xV_2O_5$ ($x < 0.01$), ϵ - $Li_xV_2O_5$ ($0.35 < x < 0.7$), δ - $Li_xV_2O_5$ ($0.7 < x < 1$), and γ - $Li_xV_2O_5$ ($1 < x < 1.9$), respectively.^{2, 25} And cyclic voltammetry (CV) of the nanocrusts (Figure S 6a) between 1.5 and 4 V was measured at a scan rate of 1 mVs⁻¹. The pairs of redox peaks can be clearly resolved in the voltage window of 1.5 – 4.0 V, which is consistent with the plateaus the discharge voltage/capacity profile. In previous studies, the electrochemical reaction between vanadium oxides and metal lithium can be described as followed:^{2, 25-28}



And the first discharge capacity of the V_2O_5 nanocrusts is more than 294 mA h⁻¹, which is more than the theoretic capacity for 2 Li^+ intercalation. The large capacity can be attributed to the nanocrusts which have a large interfacial area with the electrolyte and the defects in the V_2O_5 materials formed in the thermal decomposition of precursor. These can lead to more than two Li^+ insertion in the voltage window of 2.0 – 4.0 V. As shown in Figure S7, the discharge capacity of the V_2O_5 nanocrusts and the

V₂O₅ nanorods maintains a stable capacity around 220 and 180 mA h g⁻¹, respectively. Notably, compared to that of the commercial V₂O₅ (the discharge capacity is ~70 mA h g⁻¹), the discharge capacity of the V₂O₅ nanocrusts and the V₂O₅ nanorods are much higher.

Figure 5c shows the specific capacity of the first 50 cycles at a current density of 300 mA g⁻¹ between 2.0 and 4.0 V (versus Li⁺/Li) for commercial V₂O₅, the V₂O₅ nanocrusts and the V₂O₅ nanorods, respectively. It is illustrated that the V₂O₅ nanocrusts exhibit an initial capacity of 353 mA h g⁻¹ and 210 mA h g⁻¹ during the 1st and 30th cycle. The discharge capacity of the V₂O₅ nanorods only deliver about 160 mA h g⁻¹ after 30 cycles, which can be attributed to that the growth of V₂O₅ crystals increased the Li⁺ diffusion path length.²⁹ Although there are some loss of the capacity for the V₂O₅ nanocrusts and V₂O₅ nanorods, the capacity of V₂O₅ nanocrusts and V₂O₅ nanorods is 2-3 times of the capacity of commercial V₂O₅ after 50 cycles. The capacity loss could be attributed to the phase of crystalline V₂O₅ irreversible transition during insertion/extraction of Li⁺ ions. These cyclic performances are better than the nano-sized V₂O₅ synthesized by thermal treatment or flame spray pyrolysis.^{13, 30} The results of the V₂O₅ nanocrusts are also better than that of vanadium oxide nanobelts prepared by hydrothermal method.^{12, 20, 31, 32} Compared to other transition metal oxides such as MnO₂, Co₃O₄, the discharge capacity of as-obtained nanostructured V₂O₅ are still good as cathode materials due to its high theoretical capacity.^{1, 33}

The rate capability of the electrode materials for LIB is also an important factor for practical applications. In order to investigate the rate capability of the V₂O₅ nanocrusts and the V₂O₅ nanorods, galvanostatic cycling was carried out at various current densities. Figure 5d shows the rate performance of the V₂O₅ nanocrusts and the V₂O₅ nanorods in the voltage range of 2.0 – 4.0 V (versus Li⁺/Li) at different current densities in the range of 30–3000 mA g⁻¹. The discharges of both samples are decreased with the current density increasing. Similar to the cycle performance, the nanocrusts V₂O₅ showed a relatively enhanced rate capability compared to the nanorods V₂O₅. An initial discharge capacity of 410 mA h g⁻¹ is attained at a low current density of 30 mA g⁻¹ for the nanocrusts V₂O₅ which stabilizes at above 300 mA h g⁻¹ after 6 cycles. And the discharge capacities of the nanocrusts V₂O₅ are about 257, 237, 185 and 85 mA h g⁻¹, at 300, 600, 1000, and 3000 mA g⁻¹, respectively. Correspondingly, the nanorods V₂O₅ have values of 330, 178, 124, 89 and 21 mA h g⁻¹ at different rates of 30, 300, 600, 1000, and 3000 mA g⁻¹, respectively. Owing to inherent low electronic conductivity of V₂O₅, the discharge capacities of both samples are greatly reduced at higher current densities.² Furthermore, the discharge capacities of both samples recovered to 250 and 205 mA h g⁻¹, upon returning to a current of 30 mA g⁻¹. This illustrates that both of the structural stability and reversibility for the two samples are quite well. The rate performance of the nanocrusts V₂O₅ is better comparable to the previously reported carbon-coated vanadium oxide.^{30, 34} And these results indicate that the electrochemical property of the V₂O₅ nanocrusts and the V₂O₅ nanorods are close to the results of nano-structured vanadium oxide reported previously.^{13, 23-29} But this method is more facile and has the capable of scaling up for broad application prospects.

Conclusions

A potential method for fabrication of the V₂O₅ nanocrusts has been proposed *via* combustion of precursor from mixing commercial V₂O₅ with molten urea. And the V₂O₅ nanorods were further prepared through a controllable nanoscale growth originated from the nanocrusts during the further annealing at 630 °C. The minimization of surface energy of V₂O₅ grain probably drives the growth of the nanorods dominated by {001} surface. It is demonstrated that the discharge capacity of the as-obtained V₂O₅ nanocrusts and the V₂O₅ nanorods are raised to 210 and 170 mA h g⁻¹, respectively, from 70 mA h g⁻¹ after 30 cycle compared with commercial V₂O₅.

This work was supported by National High-tech R&D Program (863 Program, No. 2008AA03Z306), the National Natural Science Foundation of China (51003009, 21276046 and 21476045), the Ministry of Education Science and technology research projects, the Fundamental Research Funds for the Central Universities of China (DUT11LK16), (DUT13RC(3)043 and DUT14RC(3)040). We also thank Professor Zhang Xinbo (Changchun Institute of Applied Chemistry, Chinese Academy of Sciences, Changchun) for electrochemical measurements.

Notes and references

- ^a State Key Laboratory of Fine Chemicals and Faculty of Chemical, Environmental & Biological Science and Technology, Dalian University of Technology, 2 Linggong Road, High Technology Zone, Dalian 116012, P. R. China. Fax: +86-411-84986067; Tel: +86-411-84986067; E-mail: ninggl@dut.edu.cn
- ^b School of Materials Science and Engineering, Dalian University of Technology, Dalian, 116012, P. R. China.
- [†] Electronic Supplementary Information (ESI) available: Supplemental data of fourier transform infrared spectrum, thermal gravimetric analysis, electron microscopy images and cycle discharge performance see DOI: 10.1039/b000000x/
- J. Tarascon and M. Armand, *Nature*, 2001, **414**, 359–367.
 - Y. Wang and G. Cao, *Chem. Mater.*, 2006, **18**, 2787–2804.
 - H. Liu and W. Yang, *Energy Environ. Sci.*, 2011, **4**, 4000.
 - S. Batteries, S. Tepavcevic, H. Xiong, V. R. Stamenkovic, X. Zuo, and M. Balasubramanian, *ACS Nano*, 2012, **6**, 530–538; F. Wang, S. Xiao, Y. Hou, C. Hu, L. Liu, and Y. Wu, *RSC Adv.*, 2013, **3**, 13059.
 - H. Pang, Y. Dong, S. L. Ting, J. Lu, C. M. Li, D.-H. Kim, and P. Chen, *Nanoscale*, 2013, **5**, 7790–4.
 - S. Wang, Z. Lu, D. Wang, C. Li, C. Chen, and Y. Yin, *J. Mater. Chem.*, 2011, **21**, 6365.
 - M. Armand and J. Tarascon, *Nature*, 2008, **451**, 2–7.
 - T. Zhai, H. Liu, H. Li, X. Fang, M. Liao, L. Li, H. Zhou, Y. Koide, Y. Bando, and D. Golberg, *Adv. Mater.*, 2010, **22**, 2547–52; X. Rui, J. Zhu, W. Liu, H. Tan, D. Sim, C. Xu, H. Zhang, J. Ma, H. H. Hng, T. M. Lim, and Q. Yan, *RSC Adv.*, 2011, **1**, 117.
 - A. Pan, J.-G. Zhang, Z. Nie, G. Cao, B. W. Arey, G. Li, S. Liang, and J. Liu, *J. Mater. Chem.*, 2010, **20**, 9193.
 - Y. Wang and G. Cao, *Adv. Mater.*, 2008, **20**, 2251–2269.
 - X. Yu, Z. Lu, G. Zhang, X. Lei, J. Liu, L. Wang, and X. Sun, *RSC Adv.*, 2013, **3**, 19937.
 - W. Hu, X.-B. Zhang, Y.-L. Cheng, Y.-M. Wu, and L.-M. Wang, *Chem. Commun. (Camb.)*, 2011, **47**, 5250–2.
 - N. Pinna, J.-F. Hochepeid, M. Niederberger, and M. Gregg, *Phys. Chem. Chem. Phys.*, 2009, **11**, 3607.
 - H. Pang, P. Cheng, H. Yang, J. Lu, C. X. Guo, G. Ning, and C. M. Li, *Phys. Chem. Chem. Phys.*, 2013, **49**, 1536–8.

- 15 H. Li, P. He, Y. Wang, E. Hosono, and H. Zhou, *J. Mater. Chem.*, 2011, **21**, 10999.
- 16 A. M. Glushenkov, V. I. Stukachev, M. F. Hassan, G. G. Kuvshinov, H. K. Liu, and Y. Chen, *Cryst. Growth Des.*, 2008, 2–6.
- 17 C. K. Chan, H. Peng, R. D. Twisten, K. Jarausch, X. F. Zhang, and Y. Cui, *Nano Lett.*, 2007, **7**, 490–5.
- 18 Y.-C. Si, L.-F. Jiao, H.-T. Yuan, H.-X. Li, and Y.-M. Wang, *J. Alloys Compd.*, 2009, **486**, 400–405.
- 19 Y. L. Cheah, V. Aravindan, and S. Madhavi, *J. Electrochem. Soc.*, 2012, **159**, A273–A280.
- 20 B. Azambre, M. J. Hudson, and O. Heintz, *J. Mater. Chem.*, 2003, **13**, 385–393.
- 21 H. Wang, K. Huang, C. Huang, S. Liu, Y. Ren, and X. Huang, *J. Power Sources*, 2011, **196**, 5645–5650.
- 22 P. Liu, I. L. Moudrakovski, J. Liu, and A. Sayari, *Chem. Mater.*, 1997, **4756**, 2513–2520; S. Cheng, H.-D. Hwang, and G. E. Maciel, *J. Mol. Struct.*, 1998, **470**, 135–149.
- 23 X. Zhou, G. Wu, J. Wu, H. Yang, J. Wang, G. Gao, R. Cai, and Q. Yan, *J. Mater. Chem. A*, 2013, **1**, 15459.
- 24 D. C. Sayle, D. H. Gay, A. L. Rohl, C. R. A. Catlow, J. H. Harding, and M. A. Perrid, *J. Mater. Chem.*, 1996, **6**, 653–660.
- 25 C. O'Dwyer, V. Lavayen, D. a. Tanner, S. B. Newcomb, E. Benavente, G. González, and C. M. S. Torres, *Adv. Funct. Mater.*, 2009, **19**, 1736–1745.
- 26 D. Yu, C. Chen, S. Xie, Y. Liu, K. Park, X. Zhou, Q. Zhang, J. Li, and G. Cao, *Energy Environ. Sci.*, 2011, **4**, 858.
- 28 D. Fang, L. Li, W. Xu, G. Li, Z. Luo, C. Liang, Y. Ji, J. Xu, and C. Xiong, *RSC Adv.*, 2014, **4**, 25205.
- 29 X. Chen, E. Pomerantseva, K. Gregorczyk, R. Ghodssi, and G. Rubloff, *RSC Adv.*, 2013, **3**, 4294.
- 30 J. Shin, H. Jung, Y. Kim, and J. Kim, *J. Alloys Compd.*, 2014, **589**, 322–329.
- 31 X. Zhou, G. Wu, J. Wu, H. Yang, J. Wang, and G. Gao, *Phys. Chem. Chem. Phys.*, 2014, **16**, 3973–82.
- 32 L. Mai, L. Xu, C. Han, X. Xu, Y. Luo, S. Zhao, and Y. Zhao, *Nano Lett.*, 2010, **10**, 4750–5.
- 33 B. Li, H. Cao, J. Shao, G. Li, M. Qu, and G. Yin, *Inorg. Chem.*, 2011, **50**, 1628–32.
- 34 N. S. Ergang, J. C. Lytle, K. T. Lee, S. M. Oh, W. H. Smyrl, and a. Stein, *Adv. Mater.*, 2006, **18**, 1750–1753.